COBEM 2023 27TH INTERNATIONAL CONGRESS OF MECHANICAL ENGINEERING

ABCM Brazilian Society of Mechanical Sciences and Engineering
27th ABCM International Congress of Mechanical Engineering
December 04-08, 2023, Florianópolis-SC, Brazil

COB-2023-1790
DESTRUCTION AND REGENERATION PROCESS OF A LAMINAR SEPARATION BUBBLE UNDER FORCING CONDITIONS

Omar Elias Horna Pinedo
Igor Braga de Paula
Pontifical Catholic University of Rio de Janeiro
omareliashp@gmail.com
igorbra@gmail.com

Abstract. *The destruction and regeneration transient process of a laminar separation bubble (LSB) under forcing conditions is experimentally studied. The experiments were carried out in a low turbulence and close return water Channel. An adverse pressure gradient was induced by a false wall, this wall created a convergent-divergent channel, the bubble was formed on the region of an adverse pressure gradient over a flat plane. Controlled broadband disturbances of high and low amplitude are introduced with a vibration ribbon (VR) located upstream of the LSB formation region. Velocity fields were acquired using the time-resolved two-dimensional particle image velocimetry technique (PIV). The bubble forcing consists in the excitation of a wave train with alternating periods of high and low amplitude upstream to the LSB. The wave packet contains the most unstable frequency estimated in the regime of unforced LSB. In the destruction case, the high amplitude forcing inhibits the boundary layer separation and hence the formation of the LSB. In the regeneration case, a sudden change from high to low forcing amplitude allows the bubble growth up to a limiting extend. Phase locked and ensemble average were used in data acquisition and post processing data respectively. The results show differences between the time of destruction and regeneration process of a LSB. The merging and ejection of vortices were evaluated, showing similar results with those reported in the literature. The results describe in high level of detail many features of the destruction and the regeneration transient process of a LSB.*

Keywords: *Laminar separation bubble, PIV-time resolve, Merging and ejection of vortices, Controlled broadband perturbations.*

1. INTRODUCTION

The classical definition of a laminar separation bubble (LSB) was described by Tani (1964), Gaster (1966) and Horton (1968), in the presence of a strong adverse pressure gradient a laminar boundary layer separates, then transitions and reconnects as a turbulent boundary layer. The recirculation region between the separation and reattachment point is known as LSB. In many technological applications that operate at low Reynolds numbers exist favorable conditions for the formation of LSB such as unmanned aerial vehicles, turbomachinery, low-pressure turbine blades, etc. The presence of LSB may be associated with increased noise, loss of lift, increased drag, mechanical vibrations, and consequently loss of efficiency, Ducosin et al. (2016). There are a variety of conditions in which LSBs can occur, as a representative case this work focuses on the LSB that interacts with a turbulence wake, for example, those that occur in airfoil cascades, where the turbulence wake of the previous stage interacts periodically with the bubble formed in the following stage. Sudden and abrupt variations in the environmental disturbance conditions like those left by a periodic turbulent wake can cause a destruction and subsequently regeneration process of a LSB, as shown in the figure 1. To better understand this phenomenon, it is necessary to study the dynamics of a transient LSB. In the literature there are few works that study a transitory LSB. In this work the phenomenon of destruction and regeneration process of a LSB will be analyzed experimentally with a high level of detail. The destruction process will be carried out through the introduction of a high amplitude wave train that contains the most unstable frequency estimated in the quasi-stationary LSB, subsequently, the amplitude of the wave train will be abruptly decreased up to a low amplitude level, thus triggering the LSB regeneration process. The data will be acquired using the particle image velocimetry optical technique, the processing and post-processing of the data will be carried out with codes developed in-house.

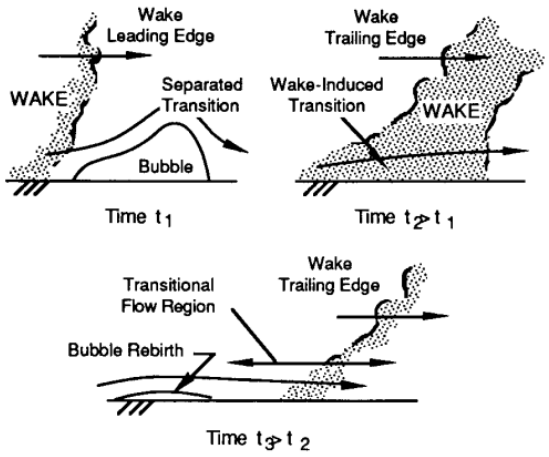

Figure 1. Schematic diagram of the effect of wake-induced transition on LSB, destruction and regeneration process of a LSB, extracted from Mayle, 1991.

2. EXPERIMENTAL SETUP

The experiments were carried out in the closed-circuit water channel of the Fluid Engineering Laboratory of the Pontifical Catholic University of Rio de Janeiro. The water channel has a test section measuring 4 x 0.86 x 0.64 m in length, width, and height respectively, the transparent glass walls of the test section provide optical access in all directions. the laminar separation bubble forms on the surface of a flat plate, the boundary layer that develops on this plate is subjected to an adverse pressure gradient generated through a false wall that together with the flat plate forms a divergent section that decelerates the flow and consequently increases the pressure, a schematic diagram of the experimental bench is shown in the figure 2.

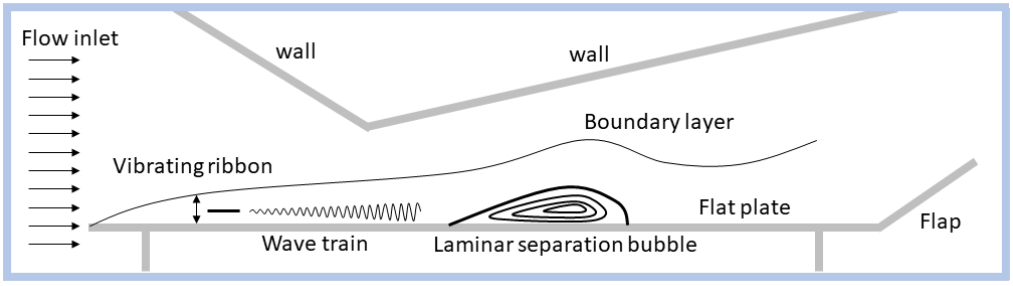

Figure 2. Schematic diagram of the test section.

The data acquisition was carried out through the particle image velocimetry technique with high temporal and spatial resolution. PIV is an optical measurement technique for measuring instantaneous velocity fields. Velocity is estimated through measurements of the displacement of groups of tracer particles dispersed in the fluid, these tracers are externally illuminated by a plane of pulsed light commonly produced by a laser source, the position of the particles is recorded by a camera at two known consecutive moments of time, image processing algorithms are used to determine the particle displacement field, as the time interval between pulses is known, then, the velocity field can be determined. A schematic diagram of the technique used in this work is shown in figure 3. A LITRON LDY-300 series system was used as a pulsed light source, two Phantom Miro 341 cameras were used to record the images, 105mm Nikkon lenses with extenders allowed to capture a measurement region of 30 x 6 cm, length by height respectively.

The data was acquired in the quasi-stationary and transient regime. For the quasi-stationary regime, a vibrating ribbon remained oscillating with low amplitude, this low amplitude oscillation has the objective of maintaining a known level of disturbance, greater than that of the environment and at the same time lower enough so that the bubble can be maintained. In the transient case, the oscillation was first of high amplitude to inhibit the formation of the bubble, then, the oscillation suddenly changed to low amplitude that allows the formation of the bubble and maintains a known disturbance level.

The geometric dimensions of the vibrating ribbon were determined from the most unstable Tollmien-Schlichting waves in the position where the vibrating ribbon is placed upstream of the LSB formation region. Thus, the width of the ribbon was chosen with a value equal to half the wavelength of TS in its operating position, that is, 13mm, and the height of the ribbon was defined as the same height at which the lowest amplitude of the TS wave is located, that is, 3 mm, this allows the minimal introduction of disturbances when the VR is stopped and maximum when it oscillates.

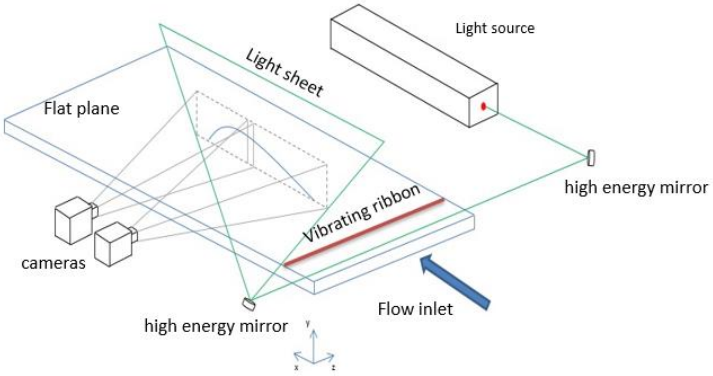

Figure 3. Schematic diagram of the configuration of the PIV system used in this work.

3. RESULTS

The results will be shown in two parts, results in stationary condition and results in transient conditions.

3.1 Quasi-steady state results

For the stationary case, an average of 5 realizations were made, each acquisition contains 2685 velocity fields, the acquisition frequency was 50 Hz and the most unstable frequency was previously identified at approximately 2.5 Hz. Figure 4 and Figure 5 show an enlarged image of the mean laminar separation bubble and some velocity profiles. These figures show the high level of detail acquired and the topological characteristics of the bubble are well defined. The bubble length is about 142mm, the Reynolds number based on momentum thickness at the separation position is 296.

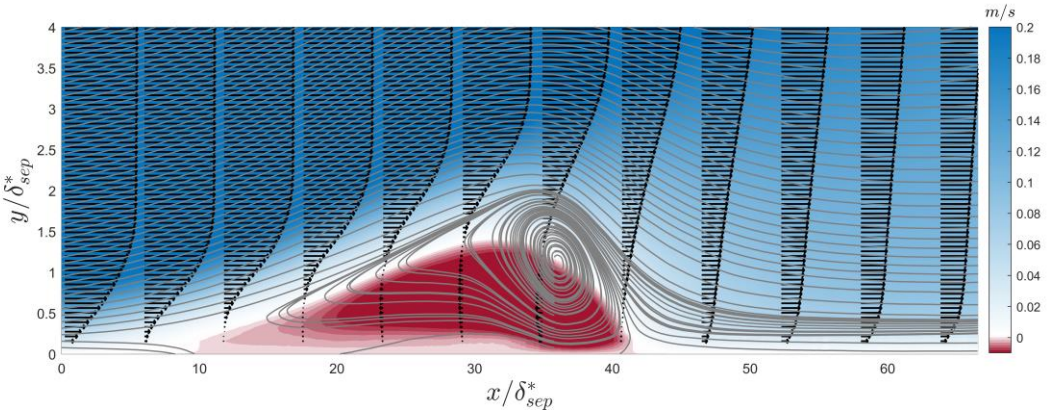

Figure 4. Colormap of streamwise velocity component and streamlines,
streamwise and wall-normal coordinates dimensionless by displacement thickness in the separation point.

The coordinates in "x" and "y" were dimensionless by displacement thickness at the separation point. In Figure 4, the reverse flow region indicated by red color is clearly observed and the core of the vortex is well defined. The maximum intensity of the reverse flow found in this work in quasi-steady conditions oscillates around 15% in relation to the local free flow velocity. This reverse flow intensity value indicates that possible absolute instability mechanisms play an important role in the bubble instability under these conditions. In the figure 5, the color map of the normal velocity component shows the bubble well defined and with an expected result, note that the core of the vortex divides the flow in two regions, one where the flow moves away from the wall and one where the flow approaches to the wall, it is precisely the approaching region indicated in color red that carries energy from the external flow to the region near the wall.

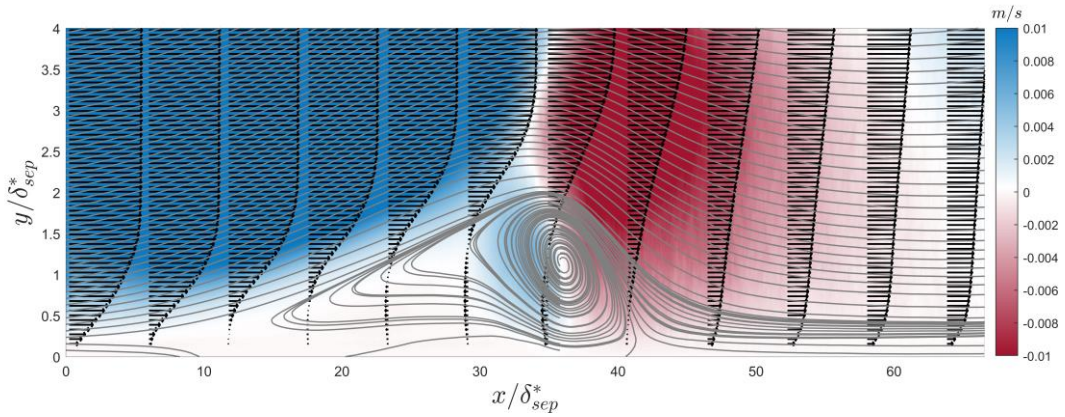

Figure 5. Colormap of wall-normal velocity component and streamlines,
streamwise and wall-normal coordinates dimensionless by displacement thickness in the separation point.

The growth of fluctuations in the quasi-stationary bubble was evaluated, it was found that the exponential growth reaches its maximum value near to the maximum height of the bubble, then saturates and decays in the turbulent region. The growth of the dimensionless power of the normal velocity fluctuation was approximately one order of magnitude greater than the streamwise fluctuations, for this reason the spectrum analysis will be performed with the normal velocity fluctuations. The growth of the dimensionless power of the velocity fluctuations can be observed in figures 6 and 7.

In quasi-stationary conditions, a power spectrum density analysis (PSD) showed that the most unstable frequency has a value of approximately 2.5 Hz. To find this value, the time series of several points were taken in the region of maximum linear growth of the fluctuations and at the same height to the displacement thickness. In figure 8 we can see the highest energy content at a frequency of 2.5 Hz.

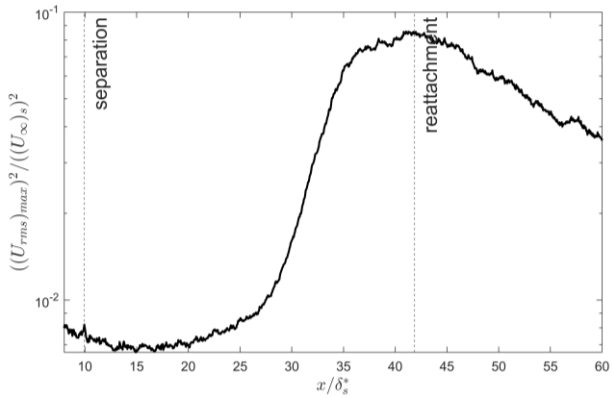

Figure 6. Dimensionless maximum power growth of streamwise velocity fluctuations,
streamwise coordinate dimensionless by displacement thickness in the separation point.

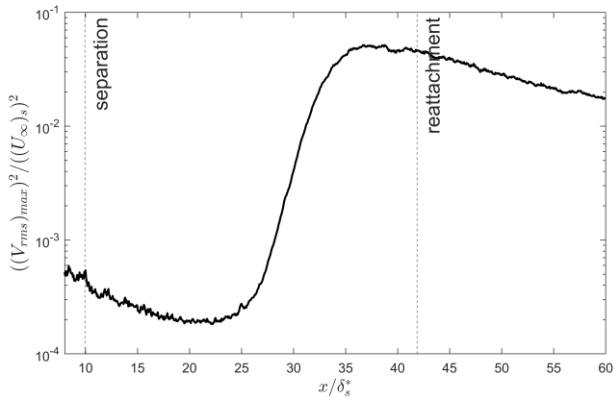

Figure 7. Dimensionless maximum power growth of wall-normal velocity fluctuations,
streamwise coordinate dimensionless by displacement thickness in the separation point.

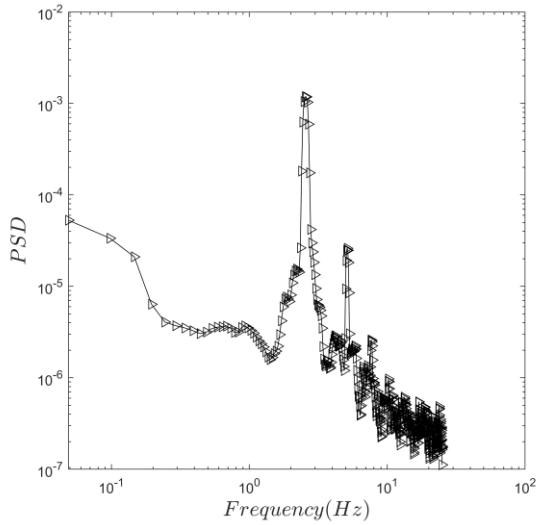

Figure 8. Power spectrum density of the wall-normal velocity fluctuations.

Using Welch's power spectral density estimate was found the spatial distribution of the energy spectral content. The most unstable dimensionless frequency is approximately St = 0.045. The energy content is confined in a narrow range, this can be associated with the modal excitation introduced by the vibrating ribbon. The spatial distribution of the energy spectral content can be seen in figure 9. Note that the highest energy content is found before the reconnection of the bubble, in the vicinity of the maximum height of the LSB.

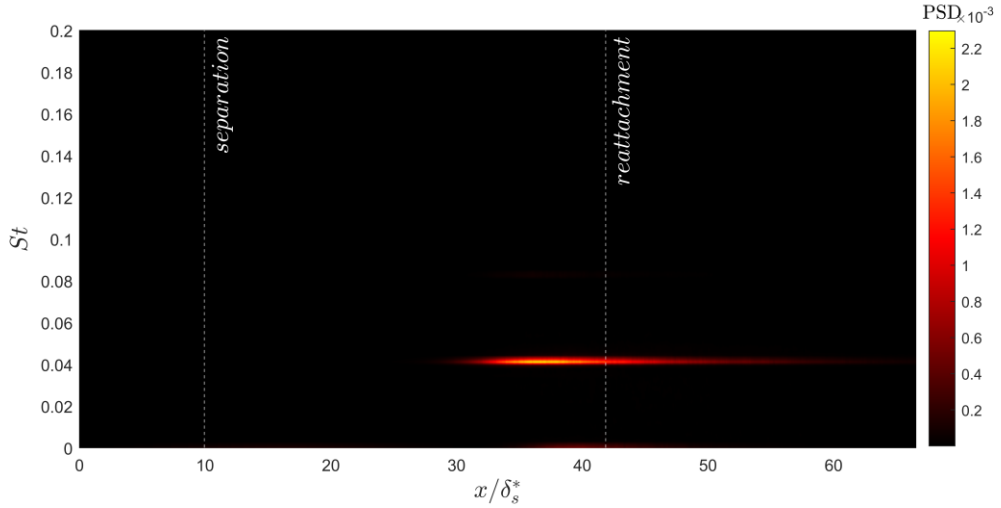

Figure 9. Spatial distribution of the energy spectral content,
streamwise coordinate dimensionless by displacement thickness in the separation point,
the vertical coordinate is the strouhal number, St.

3.2 Transient state results

The transient results were obtained from an ensemble average of 20 realizations, each realization contains 2685 velocity fields, phase locked acquired data was necessary to perform the ensemble average. The frequency of data acquisition was 50 Hz and the most unstable frequency was 2.5 Hz. The sequence of events during the bubble destruction and regeneration process is detailed.

Initially, the laminar separation bubble is in a quase-stationary state, then a high amplitude wave train is introduced into the flow through a vibrating ribbon located upstream of the bubble formation region. This wave packet contains the most unstable frequency calculated in the unforced condition. Figure 10, shows the transitory process of destruction of the LSB. Data acquisition started at t = 0 s, the time count starts with the destruction process of the LSB and continues until the complete regeneration of the LSB. At t = 0.2 s the bubble is still in its quase-stationary state, during this fraction of time the wave packet is traveling from the upstream position where the wave train was generated by the vibrating ribbon until the stationary position of the bubble, when t = 1.6 s the laminar separation bubble feels the effects of the high amplitude wave train and begins to contract, when t = 2 s there is still a separate boundary layer with a small area, when t = 2.6 s and t = 3.0 s there is no more separation of the boundary layer and the LSB stops forming (destruction), from t = 4 s onwards there will be no more formation of the LSB until the vibrating ribbon stops acting.

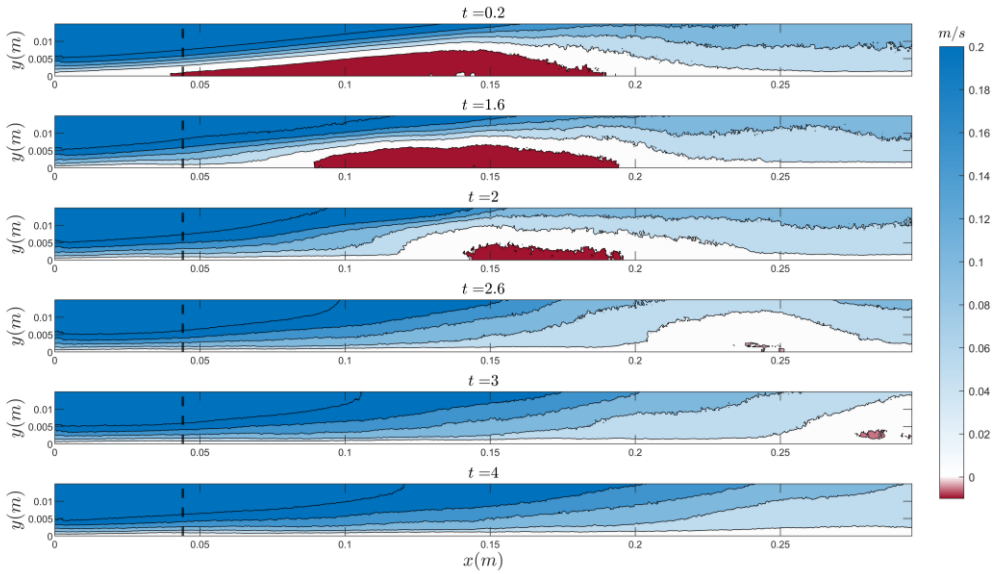

Figure 10. Destruction process of a LSB, the dashed line indicates the mean position of the separation point, the colormap represents the streamwise velocity component.

For approximately 15 seconds the vibrating ribbon introduces high amplitude disturbances, after that the amplitude of the wave train is dramatically decreased, and then the vibrating ribbon introduce a low amplitude wave train, this is done in order to generate an LSB with a known and controlled disturbance condition. Once the vibrating ribbon oscillates with low amplitude, the bubble regeneration process can begin.

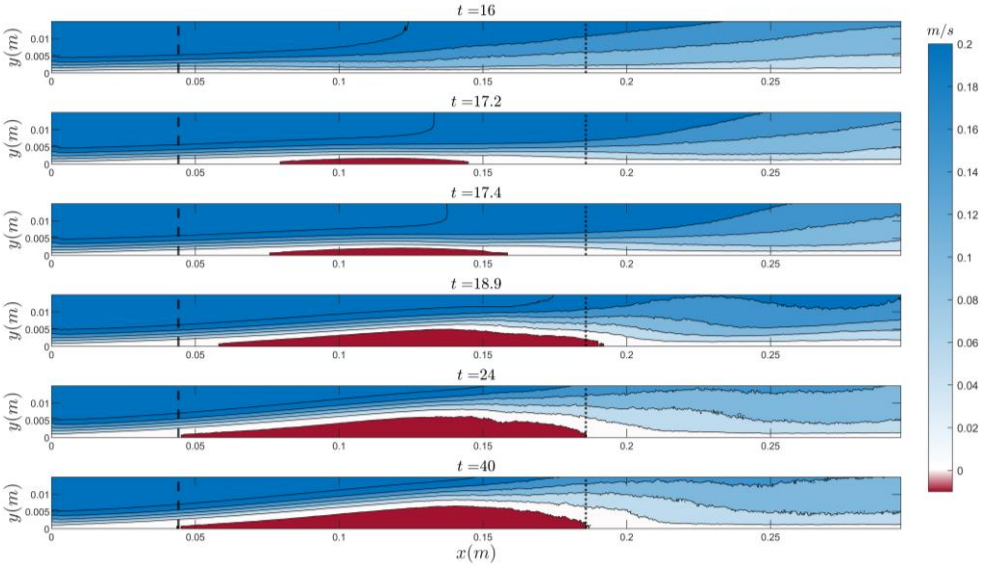

Figure 11. Regeneration process of a LSB, the dashed line indicates the position of the mean separation point, the dotted line indicates the position of the mean reattachment point, the colormap represents the streamwise velocity component.

As shown in figure 11, when t = 16 s the boundary layer continues without separating, even though the vibrating ribbon was deactivated in the second t=15 s, remaining disturbances still travel convectively towards the bubble. In t = 17.2 s and 17.4 s the boundary layer separates and grows in height and length, when t = 18.9 s the boundary layer grows abruptly and expands beyond its mean reattachment point, in this condition the LSB begins to eject vortices and immediately after the bubble begins to contract, when t = 24 s the LSB reaches its quase-stationary condition and maintains its topological characteristics in a mean sense, when t = 40 s, it can be verified that the LSB continues to maintain its mean topological characteristics. If we compare figures 10 and 11 we will verify that the length and height of the regenerated quasi-stationary bubble is similar than the initial bubble.

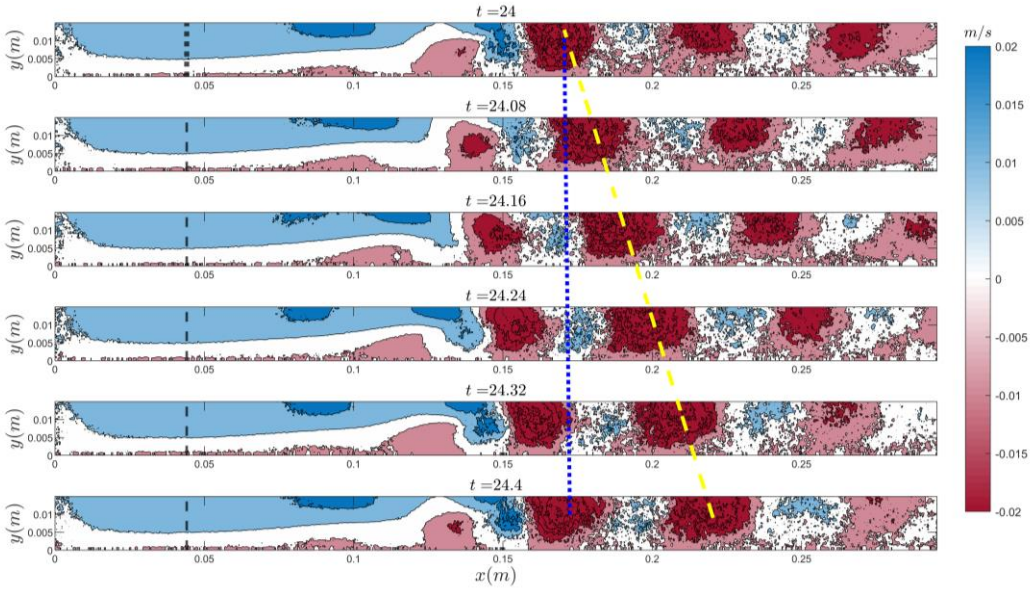

Figure 12. A single period of vortex shedding, the dotted blue line indicates the beginning and end of the period, the dashed yellow line indicates the displacement of the vortex (not the vortex core), the colormap represents the wall-normal velocity component.

Vortex shedding produces a periodic train with regions of positive and negative normal velocity component as shown in figure 12, the blue color scale represents the positive normal velocity component, and the red color scale the negative normal velocity component. the core vortex is located between these two regions. An analysis of a single period of vortex shedding showed that the wavelength of the ejected vortices has an approximate value of 5 cm. The period of this oscillation is approximately 0.4 s. In this case the frequency of vortex shedding coincides with the most unstable frequency

4. FINAL REMARKS

The results found show in a high level of detail the topology and characteristics of the LSB, some important analyzes were carried out. The most unstable frequency was identified, the evolution of the transient destruction and regeneration process was examined, results similar to those reported in the literature were found, however an important contribution of this work is the analysis of the formation process of the bubble, these results are still being the subject of analysis and discussion

5. REFERENCES

Tani, 1964. Low-speed flows involving bubble separations, Prog. Aerosp. Sci. 5, 70.

Horton, 1968. Laminar separation bubbles in two and three dimensional incompressible flow. PhD. Thesis, University of London, London

Gaster M., 1967. The structure and behavior of laminar separation bubbles. Tech. Rep. Aeronautical Research Council Reports and Memoranda 3595, London

Ducosin A, Loiseau J. Ch., 2018. Numerical investigation of the interaction between laminar to turbulent transition and the wake of an airfoil, European Journal of Mechanics B/Fluids 57, 231-248

Mayle, R.E. and Dullenkopf, K., 1989, A theory for wake-induced transition, J. Turbomachinery, 112, pp. 188-195

6. RESPONSIBILITY NOTICE

The authors are the only responsible for the printed material included in this paper.